

# A Review: Person Identification using Retinal Fundus Images

Poonguzhali Elangovan, and Malaya Kumar Nath

**Abstract**—In this paper a review on biometric person identification has been discussed using features from retinal fundus image. Retina recognition is claimed to be the best person identification method among the biometric recognition systems as the retina is practically impossible to forge. It is found to be most stable, reliable and most secure among all other biometric systems. Retina inherits the property of uniqueness and stability. The features used in the recognition process are either blood vessel features or non-blood vessel features. But the vascular pattern is the most prominent feature utilized by most of the researchers for retina based person identification. Processes involved in this authentication system include pre-processing, feature extraction and feature matching. Bifurcation and crossover points are widely used features among the blood vessel features. Non-blood vessel features include luminance, contrast, and corner points etc. This paper summarizes and compares the different retina based authentication system. Researchers have used publicly available databases such as DRIVE, STARE, VARIA, RIDB, ARIA, AFIO, DRIDB, and SiMES for testing their methods. Various quantitative measures such as accuracy, recognition rate, false rejection rate, false acceptance rate, and equal error rate are used to evaluate the performance of different algorithms. DRIVE database provides 100% recognition for most of the methods. Rest of the database the accuracy of recognition is more than 90%.

**Keywords**—Biometric, fundus image, recognition, vascular features

## I. INTRODUCTION

THERE is a huge demand for stable, reliable, and authentic person identification system as the world is manifested to threats and insecurities due to advancements in technologies. Person can be identified based on PIN (license number), biographical attributes (address, education, profession) and biological attributes [1-3]. Out of them biometrics based recognition provides better security and safety compared to the traditional methods of recognition. Biometrics refers to the automatic recognition of an identity by measuring a particular physical or behavioral characteristic. It recognizes the identity of an individual based on the extracted features. With the rapid growth of information technology, there is always a need for providing high security in digital security systems. Therefore, it is essential for a biometric system is to be secure, accurate, fast, and low cost. Fingerprint, signature/handwriting, face, iris, voice, sclera, hand geometry, and hand vein etc. are the most commonly used biometric identifiers. The strength of biometric authentication is that it cannot be lost or forgotten, as

Poonguzhali Elangovan and Malaya Kumar Nath are with Department of Electronics and Communication Engineering, National Institute of Technology Puducherry, Karaikal, INDIA (e-mail: epoonguzhali3@gmail.com, malaya.nath@gmail.com).

the person has to be physically present during the identification process. So, it is inherently more reliable, stable and capable than traditional knowledge-based and token-based authentication techniques. A brief description of biometric recognition methods is discussed below.

Identification of an individual by using their signature is termed as signature recognition [1]. Signature is a behavioural trait and may change over time and thus does not provide long-term reliability. This method has lack of accuracy and it can be easily forged.

Fingerprint recognition [2] refers to the identification of an individual by extracting relevant fingerprint features such as basic patterns and minutiae features. The basic modules of fingerprint recognition include fingerprint sensing device, pre-processing, feature extraction, and matching. Fingerprints can be spoofed easily.

Human voice is a combination of physical and behavioural biometric which is used in voice recognition [3]. Voice recognition uses unique acoustic properties for identifying an individual. Though the physical features of voice are invariant, the behavioural part changes over time. It is difficult to recognize a person suffering from cold or some throat related problems.

Facial characteristics are analyzed in face recognition [4]. It comprises of face detection, feature extraction, and matching. These algorithms mainly focus on measuring the key features of the human face. It can be spoofed easily. It hardly detects the identical twins.

Iris recognition [5] has been found to be more reliable and accurate authentication system and mainly used in high profile applications. The thin and circular structure present in the human eye is iris. Iris patterns are highly unique and cannot be spoofed or modified. It fails in case of affected eyes due to haziness of iris patterns.

Sclera recognition [6] mainly utilizes the blood vessel patterns present in the sclera for authentication purpose. Sclera is considered as the highly protected portion of the human eye, consists of various tissues. The main modules of sclera recognition are sclera segmentation, sclera vessel feature extraction and feature matching. It is very difficult to capture a complete sclera image. Also, the appearance of texture patterns can change due to different lighting conditions.

Above mentioned recognition techniques are having a lack of security. Therefore, it is essential to consider a biometric characteristic which is unique, stable and be easily measurable. This leads to the development of a retina based authentication system. Human retina has no contact with the external environment and hence, it is not prone to external

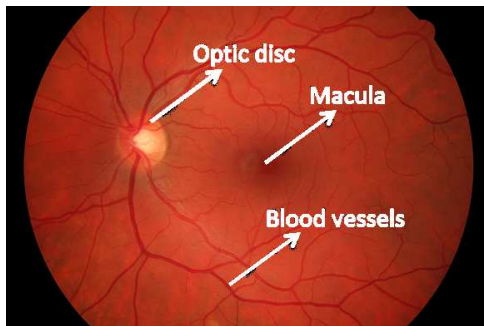


Fig. 1. Normal fundus image

changes and impossible to forge. Retina remains stable in ones lifespan. Uniqueness in vascular pattern lying over retina is the foundation of retina recognition. Uniqueness of retinal vascular pattern was discovered by Dr. Carleton Simon and Dr. Isodore Goldstein [7]. Later it was found to be unique in case of identical twins by Dr. Paul [8]. Retinal vascular patterns remain unaltered throughout a persons lifetime unless the person undergoes some severe eye surgery or injury [9]. Moreover, the feature vector size is smaller compared to other biometric feature vectors. This results in faster recognition. Therefore, the retina can be considered as the most accurate biometric among all other biometric traits. It also overcomes computer-based frauds such as hacking and identity theft, as an individuals biometric data is unique and non-transferable.

The main features of fundus image which is captured by a digital fundus camera include optic disc, blood vessels, and macula are shown in Fig.1 [10]. Among the retinal features, the most prominent feature for retina based person identification is the blood vessel. Blood vessels form a tree shaped branched network pattern with optic nerve head as root over the retinal surface.

Several retinal recognition methods have been published in the last few years. The methods have been discussed and compared in this paper. The organization of the paper is as follows: Section 2 covers, the different retina based person identification methods along with the results obtained by various authors. Discussion about Retinal databases and performance measures are discussed in Section 3. Finally, Section 4 provides the conclusions.

## II. TECHNIQUES

Person identification using human retina can be broadly classified into two methods such as vascular based and non-vascular based [11]. Vascular based method uses blood vessel properties of retinal images, whereas non-vascular based methods aim to analyze the non-vessel properties of the retinal images. Retina based person identification mainly consists of enrollment module and identification module as shown in Fig.2. The digital fundus image is applied as an input to this authentication system. Enrollment module includes pre-processing, blood vessel segmentation, feature extraction, and feature matching. Pre-processing is the first module of enrollment and it consists

of contrast enhancement, background elimination, blood vessel enhancement, region of interest (ROI) identification, optic disc localization, and image center calculation.

Different blood vessel segmentation techniques such as adaptive thresholding, matched Gaussian filtering, multiscale line detection, supervised multilayered thresholding, and morphological operation are used in the literature for the extraction of vascular features. Non-vascular features are extracted from the original fundus image. A feature vector is generated from the extracted features. A database is created by applying image processing techniques to various images. In an identification module, the feature vector of the query/test image is formed by applying the same image processing techniques. The resultant feature vector is compared with the database feature vectors by using a suitable similarity matching method. Euclidian and Mahalanobis distance measures are the most widely used methods for finding the similarity between the test image and trained images. Identity as genuine or imposter is established based on the matcher output.

### A. Vascular based methods

Vascular based methods mainly utilize the blood vessel pattern of the fundus image shown in Fig.3. The unique property of the blood vessel network is employed in this method. An accurate and efficient blood vessel segmentation algorithm is essential for this approach. Several research work has been implemented in the past for blood vessel segmentation from the fundus image [12]. Vascular based person identification comprises of various stages such as image pre-processing, blood vessel segmentation, feature extraction, and feature matching. Bifurcation point, branch point, end point, crossover point, and blood vessels inside the optic disc region are the relevant vascular features. Fig.4 shows the relevant blood vessel features.

a) *Bifurcation point* is a point at which bifurcation of a blood vessel takes place. It splits the vessel into two separate vessels.

b) At *branch point* new minor vessel comes out from the major or wider vessel.

c) Two vessels cross each other at *crossover point*.

d) *End point* is the termination of blood vessel.

e) *Blood vessels inside optic disc* is the stable and unique blood vessel pattern.

Different algorithms have been implemented by researchers in the past few years for person identification using vascular features. Farzin et al. [13] utilized blood vessel features around the optic disc region for identification. The proposed system includes blood vessel segmentation, feature generation, and feature matching. Blood vessel segmentation includes various steps such as OD localization, brightness reduction of OD, contrast enhancement, and histogram thresholding. A template matching technique is used to locate the optic disc center. First, a template is generated by averaging various rectangular region of interest (ROI) in the database. The template is correlated with the green component image and the brightest pixel in the correlated image is identified as OD center. The undesired brightest effect of OD is suppressed by performing a pixel

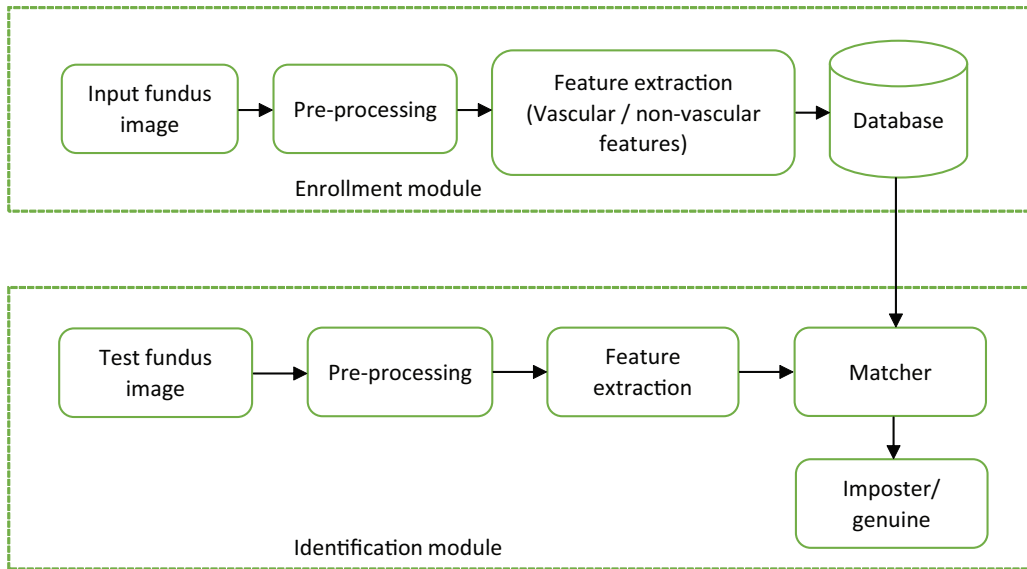


Fig. 2. Block diagram of retina based person identification system

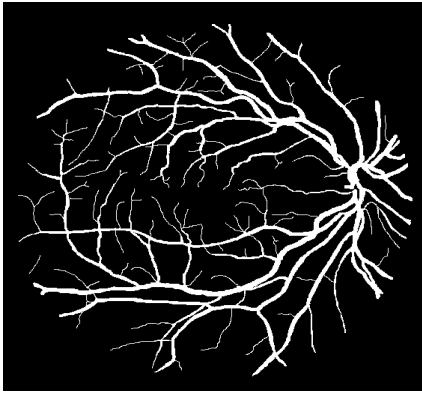


Fig. 3. Vascular network

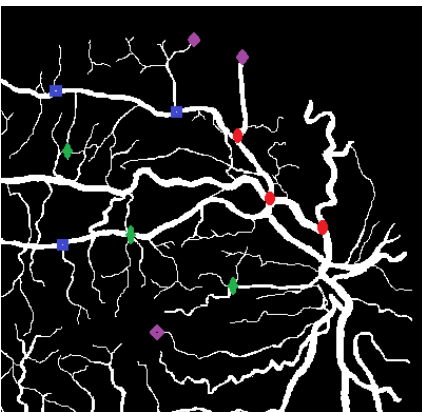


Fig. 4. Bifurcation point (red), branch point (blue), crossover point (green) and end point (violet)

by pixel division of the original image by the correlated image. Local contrast and morphological contrast enhancement techniques are used to enhance the blood vessels. A sliding window is employed to obtain a contrast enhanced image in local contrast enhancement technique. As a result of the small window size, large vessels are transformed into two parallel curves. This problem is rectified by applying morphological dilation and erosion operations. Then histogram thresholding method is used to extract the blood vessels from the enhanced image. Several steps such as vessel masking, polar transform, multiscale analysis, and feature vector formation are carried out in feature extraction block. The blood vessels present in the vicinity of optic disc region is extracted using a ring mask, centered at OD location. In order to obtain rotation invariant image, polar transform is applied on the binary ROI image. Multiscale analysis of a polar image is carried out in three scales using discrete stationary biorthogonal wavelet transform. The residual coefficients of large, medium and small blood vessels are obtained. The residual coefficients in the third scale are thresholded to extract the large vessels. Large vessels are removed from the polar image in order to obtain medium vessels. A suitable threshold is used to extract the medium vessels from the residual coefficients of the wavelet transform in the second scale. This is followed by small vessels extraction by removing the large and medium vessels from the polar image. The vessel position and orientation in each scale are used to generate a feature vector. In feature matching block, modified correlation (MC) between the feature vectors is calculated using

$$MC_i(\phi) = \sum_{\tau=1}^N \text{step}(\theta_i(\tau) * \theta_i^q(\tau + \phi)) * \cos[\alpha * (\theta_i(\tau) - \theta_i^q(\tau + \phi))], i = 1, 2, 3, \quad (1)$$

where  $\theta_i$  is the feature vector of enrolled image,  $\theta_i^q$  represents the feature vector of test image,  $\tau$  is the circular

translation value,  $N = 360$  is the length of the feature vector in each scale, and  $\alpha$  is a coefficient set to 1.7. A new similarity index is then computed based on the maximum MC value. The algorithm is tested on DRIVE and STARE database, and an average equal error rate of 1% is achieved in both the databases.

Usman et al. [14] have proposed four stage retinal identification system, which consists of pre-processing, vascular pattern recognition, feature extraction, and biometric pattern matching. Background subtraction and noise removal are performed in pre-processing stage to avoid any false detection of feature. Green component of the fundus image is considered for background elimination. Authors have used gradient mean and variance based method to achieve this. The noise present in the retinal image is removed by considering the HSI (Hue, Saturation, and Intensity) color space. The blood vessels are enhanced using 2D Gabor wavelet and extracted using adaptive thresholding in the second stage. With suitable scale value, Gabor wavelet transform is computed for each pixel location and the maximum value is taken. The Gabor wavelet coefficients can be computed using

$$\varphi_G(x) = \exp(jk_0x) \exp\left(-\frac{1}{2}|Ax|^2\right), \quad (2)$$

where  $k_0$  is a vector that defines the frequency of the complex exponential and  $A$  is an elongation diagonal matrix in any desired direction. This results in an enhanced vascular network. The optimum threshold value needed to minimize the intra-class variance is computed using an adaptive thresholding algorithm. The blood vessels are extracted by using this optimum threshold value. This is followed by morphological thinning operation. Bifurcation points are extracted and filtered in the third stage. Feature extraction is performed by using crossing number (CN) method defined by

$$C(p) = \frac{1}{2} \sum_{i=1}^8 |f_{thin}(p_{i \bmod 8}) - f_{thin}(p_{i-1})|, \quad (3)$$

where  $f_{thin}$  is the thinned image and  $p_i$  represents the pixel values. This method extracts the bifurcations by examining the local neighborhood of each ridge pixel using a  $3 \times 3$  window. The false bifurcation points are eliminated using a window method. The relative angles and distances between each bifurcation point and its four nearest bifurcation points are calculated in order to make matching invariant to translation and rotation. The template feature vector is created for each bifurcation point. Finally, matching using Euclidian distance is performed between the stored features and features acquired from the test image. The recognition rate of 100%, 95.06%, and 99.14% is achieved in DRIVE, STARE and VARIA databases, respectively. The recognition rate is comparatively lower in STARE database as it contains 51 images with severe eye disease, which prevent the complete extraction of feature points.

Fatima et al. [15] developed a three stage system for retinal person identification. Blood vessel enhancement and segmentation are performed in the pre-processing stage. Gabor wavelet defined in Equation (2) with a scale value of four

is applied to the green channel image for enhancement of blood vessels. The maximum wavelet response from eighteen different wavelet responses is selected for every pixel. Then a recursive supervised multilayered thresholding technique is employed to segment the blood vessels. This is followed by morphological thinning operation in order to make vessel width equal to single pixel. Thus a neat thinned blood vessel pattern is extracted in the pre-processing stage.

Extraction of vascular features and feature validation are done in the feature extraction stage. Crossing number method given in Equation (3) is employed to extract the bifurcation point. The value  $C(p) = 3$  indicates bifurcation point and  $C(p) = 1$  indicates end point. A windowing technique is utilized to remove the falsely identified feature points. Each feature point is represented by a feature set consisting of relative angles and relative distances between the feature point and its four nearest feature points. Finally, matching is performed using Mahalanobis distance measure. The similarity between the two retinal images is computed by a score value. They tested their algorithm on VARIA and RIDB databases and obtained the recognition rate of 99.57% and 97%, respectively.

Ritesh et al. [16] have proposed a 7 state Hidden Markov model (HMM) based person identification system. The flow diagram of the proposed method is given in Fig.5. Initially, the blood vessels are segmented by applying filtering and thresholding operations in the green plane image. The matched filter with first-order Gaussian derivative is used for blood vessel extraction. The retinal vascular region is partitioned into seven sub-regions like terminal branching upper, secondary branching upper, primary branching upper, optic disc region, primary branching lower, secondary branching lower, and terminal branching lower based on 1D Hidden Markov model. Every partitioned region has a unique state in HMM representation. SVD provides an efficient way of extracting features from the image in an algebraic manner. The retinal images are resized to  $46 \times 56$  in order to reduce the computational complexity. The uncorrelated features about the cup and disc are represented by SVD coefficients. The final feature vector is created by considering the larger singular values as they contain more image information. This is followed by the quantization of continuous SVD values. Each quantized vector and each of the sub-image block has a unique integer value. This results in a mapping of the retinal image into a series of observation vectors. Finally, the images are interpreted as a 1D sequence of vectors, followed by HMM-based classification. Authors have obtained recognition rate of 95%, 85.33%, and 100% in DRIVE, glaucoma, and ARIA databases, respectively.

Fig.6 shows the identification method proposed by Waheed et al. [17] with an improved blood vessel segmentation algorithm. First, blood vessels are enhanced by 2D Gabor wavelet. A recursive supervised multilayered thresholding based method is employed to segment the blood vessels. This is followed by vessel validation which includes region based extraction and classification. Morphological properties of true and false vessels are employed to remove the false vessels from the vessel map. To achieve this, region based features such as Euler number, eccentricity, convex area, filled area, major axis length, minor axis length, and solidity are extracted.

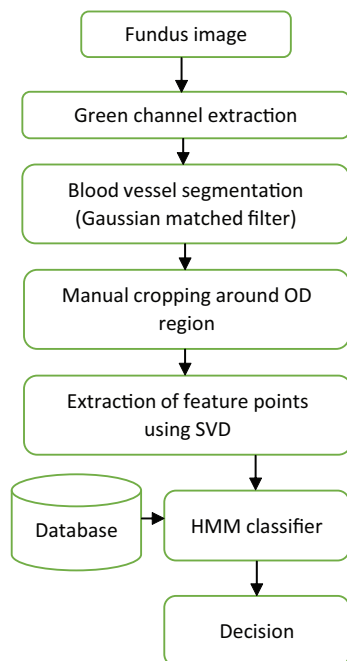


Fig. 5. Flow diagram of algorithm proposed by Ritesh et al. [16] (2014)

Intensity based features like maximum intensity, minimum intensity, and mean intensity are also extracted. These features are used to obtain a neat vessel map with the help of SVM classifier. Each vascular region is classified into true and false vessels by SVM classifier.

In the feature extraction phase, minutiae points are extracted from the blood vessel map using crossing number method given in Equation (3). Then the required rotation and translation invariant feature vectors are computed. The similarity between the query feature vector and enrolled feature vectors are calculated using cosine similarity index matching. The cosine similarity between the two vectors is mathematically represented by

$$\text{ConSim}(x, y) = \frac{x \cdot y}{\|x\| \|y\|}. \quad (4)$$

The final decision is made based on the highest score value. Authors have obtained recognition rate of 100% and 78.57% on RIBD and DRIBD databases, respectively.

Jiu et al. [18] identified the person using vascular pattern. Blood vessel enhancement and segmentation are performed in pre-processing stage. The 2D Gabor wavelet defined in Equation (2) is used to enhance the blood vessels. With varying rotation angles from 0 to 170 degrees, Gabor wavelet is computed for every pixel and the maximum response is considered. Adaptive thresholding technique is used to segment the blood vessels from an enhanced image. Morphological thinning operation results in a uniform thickness of blood vessels. Feature extraction is performed by crossing number method. Bifurcation and end points are extracted from the segmented blood vessel map. Then, feature validation algorithm is used to eliminate the falsely detected features. To achieve this, authors have used windowing technique with different window sizes such as  $5 \times 5$ ,  $7 \times 7$ , and  $9 \times 9$ . The feature vector is formed

based on the extracted features. Euclidean distance between query vector and stored vector is used for matching. They have obtained an accuracy of 100%, 95.06%, 98.28% on DRIVE, STARE, and VARIA databases, respectively.

In 2015, Bhuiyan et al. [19] has proposed the retinal person identification system consists of enrollment or registration stage and verification stage. The block diagram is shown in Fig. 7. In registration or enrollment phase blood vessel extraction and centerline detection are performed for identification of vascular branch, bifurcation and crossover points from the captured retinal image. Blood vessel segmentation is performed using multiscale line detection technique [20]. This method is very effective, as it combines line detectors with varying scales to produce an enhanced image from which blood vessels are segmented by suitable threshold. Region filling operation is applied to remove the artifacts (black regions) present in the blood vessels. Then vessel centerline image is obtained using morphological operation.

The wider vessels are identified by applying vessel width measurement method. To achieve this, the coordinates of all the pixels present in the vessel centerline are obtained. These pixels are mapped in pair-wise and for each pair, a perpendicular line is considered. Then by counting the total number of white pixels lying on the perpendicular line, vessel width is calculated. Extraction of feature points and feature vector generation is done in feature extraction stage. Branch, bifurcation, and crossover points are extracted from the wider vessels. A model with these features is developed using geometric hashing technique, which is a powerful technique used to obtain a unique pattern of the feature points. The resultant pattern is invariant to translation, rotation, and scaling. Recognition is made by comparing the query model with predefined models in the database. For local database, the algorithm provides the precision value to be 96.64% and recall 100%, respectively.

Results obtained considering the feature points of blood vessel network are tabulated in Table I. Various performance measures such as accuracy (AC), recognition rate (RR), precision (PR), recall (RE), equal error rate (ERR), false acceptance rate (FAR), and false rejection rate (FRR) have been used by the authors. Waheed et al. [17], Usman et al. [14], Jiu et al. [18], and Ritesh et al. [16] have obtained the recognition rate of 100% by using vascular based method for person identification on RIBD, DRIVE, and ARIA databases respectively. Some cases the recognition rate is low due to pathologies.

### B. Non-Vascular based methods

Non-vascular based methods utilize the structural properties of fundus image for recognition. Since the features are extracted from the original retinal image, blood vessel segmentation is not required. Very few works of literature are available for person identification using non-vascular features. Some authors have used statistical and texture features for identification. Researchers have also utilized corners of retinal fundus image as features. Most commonly used non-vascular features are corner points, statistical features, texture features, Fourier coefficients, moment based features, luminance, and contrast.

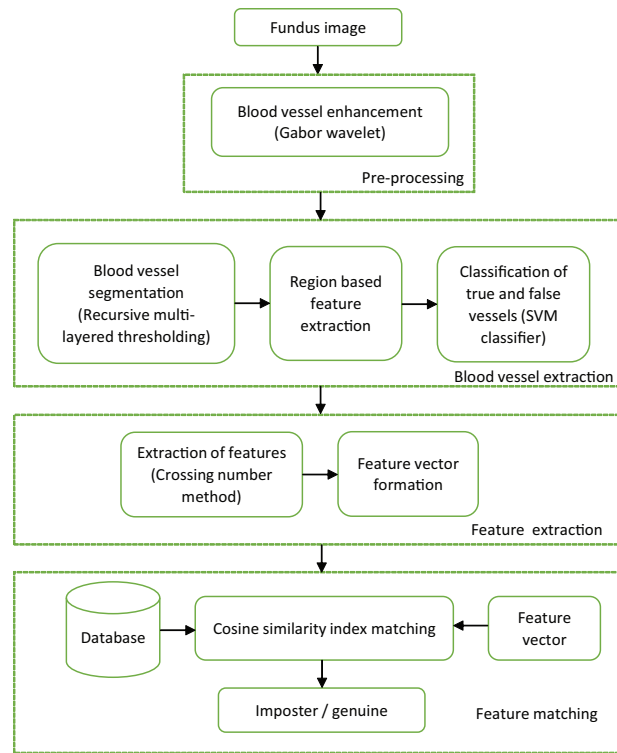


Fig. 6. Flow diagram of algorithm proposed by Waheed et al. [17] (2016)

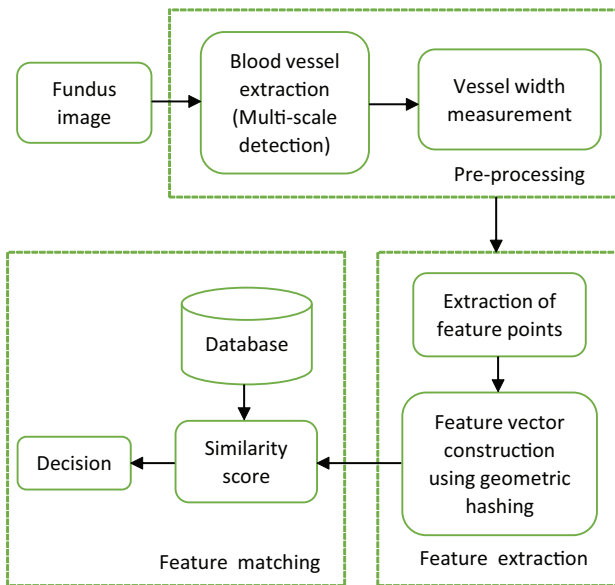


Fig. 7. Flow diagram of algorithm proposed by Bhuiyan et al. [19] (2017)

Rahman et al. [21] have proposed a method for person identification based on the non-vascular features extracted from the retinal fundus image. The flow diagram is given in Fig.8. The pre-processing stage includes background elimination, contrast enhancement, and ROI identification. A thresholding technique is applied on the red channel in order to eliminate the background noise. The contrast of intensity image is enhanced by local contrast enhancement method. The region around an optic disc center with size  $110 \times 100$  is identified as the region

of interest. A total of thirty-two features are extracted in the feature extracting phase. Twelve statistical features (such as mean, standard deviation, skewness, and kurtosis from each color space) and twenty texture features (such as energy, entropy, correlation, contrast, and homogeneity) are extracted. The similarity score between the stored images and test image are evaluated using Euclidean distance classifier in the matching phase. Identification is performed based on the highest similarity score index value. The performance of this method varies with the threshold. Authors have noted maximum 94.5% accuracy (in threshold range 0.01 to 0.27) by testing on the database consists of sixty images. This method may not provide desired detection level in presence of pathological factors.

Sabaghi et al. [22] have proposed a robust person identification system that incorporates the rotation compensation to overcome the problem due to the anatomic movement of head or eye in image acquisition process. In order to develop a robust system, Sabaghi et al. incorporated the desired compensation in their proposed algorithm. Fig.9 shows the flow diagram for the proposed method by Sabaghi et al. which consists of rotation compensation, feature extraction, and feature matching. First optic disc center is located by a template matching technique from the green channel image. Then for an image  $I(x, y)$  with size  $M \times N$ , the center is computed using

$$x_o = \frac{\sum_{x=1}^M \sum_{y=1}^N xI(x, y)}{\sum_{x=1}^M \sum_{y=1}^N I(x, y)}, y_o = \frac{\sum_{x=1}^M \sum_{y=1}^N yI(x, y)}{\sum_{x=1}^M \sum_{y=1}^N I(x, y)}. \quad (5)$$

TABLE I  
COMPARISON OF VASCULAR BASED METHODS FOR PERSON IDENTIFICATION

Author	Techniques employed	Database	Performance measure (%)
Farzin et al. [13], (2008)	Template matching, polar transform, wavelet transform, thinning, Mahalanobis distance measure	DRIVE STARE	average EER $\simeq 0$ average EER $\simeq 0$
Usman et al. [14], (2011)	Gabor wavelet, adaptive thresholding Euclidian distance measure	DRIVE STARE VARIA	AC: 100 AC: 95.06 AC: 99.14
Fatima et al. [15], (2013)	Gabor wavelet, multilayered thresholding, thinning, Mahalanobis distance measure	VARIA RIDB	RR: 99.57 RR: 97
Ritesh et al. [16], (2014)	Matched Gaussian filter, singular value decomposition, Hidden Markov Model	DRIVE ARIA	RR: 95 RR: 100
Waheed et al. [17], (2016)	Gabor wavelet, supervised multilayered thresholding, cosine similarity matching	RIDB DRIDB	RR: 100 RR: 78.57
Jiu et al. [18], (2016)	Gabor wavelet, adaptive thresholding, thinning, Euclidian distance measure	DRIVE STARE VARIA	AC: 100(%) AC: 95.06 AC: 98.28
Bhuiyan et al. [19], (2017)	Multi-scale line detection, geometric hashing	Local	PR: 96.64 RE: 100

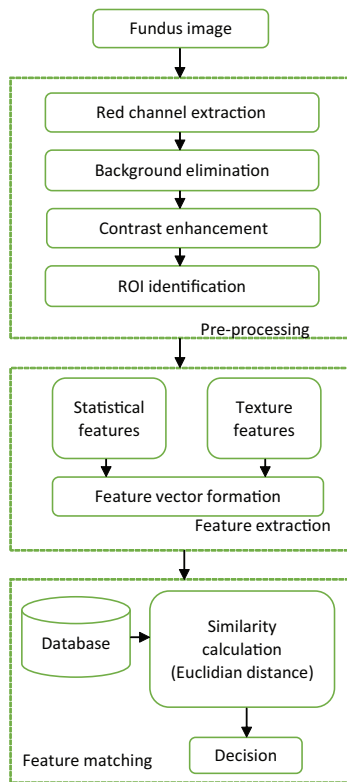


Fig. 8. Flow diagram of algorithm proposed by Rahman et al. [21] (2008)

The angle between baseline and line connecting image center point and OD center point is measured and is used for rotation compensation. The feature extraction phase includes two main steps. In the first step, Fourier energy feature (FEF) vector is calculated by performing angular partitioning on magnitude spectrum. The magnitude spectrum of the retinal

image is computed by applying 2D Fourier transform. A new partitioning is introduced by dividing the spectrum into several half circles with radius ranging from 5 to 105 pixels. The energy of each partition is computed using

$$E = \sum_{u=l_1}^{l_2} \sum_{v=k_1}^{k_2} (F_p(u, v))^2, \quad (6)$$

where  $F_p(u, v)$  represents a partition of Fourier spectrum. This is followed by the calculation of normalized FEF vector. Wavelet energy feature (WEF) vector is computed in the second step using Haar wavelet. The approximation, horizontal, vertical, and diagonal detail coefficients of  $K$ -th level decomposition are computed. The wavelet energy at  $i^{th}$  level in different directions are computed by

$$E_H = \sum_{x=1}^M \sum_{y=1}^N (H_i(x, y))^2 E_i^v \quad (7)$$

$$E_V = \sum_{x=1}^M \sum_{y=1}^N (V_i(x, y))^2 E_i^d$$

$$E_D = \sum_{x=1}^M \sum_{y=1}^N (D_i(x, y))^2,$$

where  $H_i$ ,  $V_i$ ,  $D_i$  represents the horizontal, vertical, and diagonal coefficients at  $i^{th}$  level, respectively. The calculated energies in required directions is used to create the feature vector. Normalization of the feature vector by total energy results in WEF vector. Finally, FEF and WEF vectors of the query image are compared with previously registered values available in the database. A person is identified based on a minimum Euclidean distance value. They have obtained an identification rate of 95.4%, 97.2% and 99.1% on DRIVE

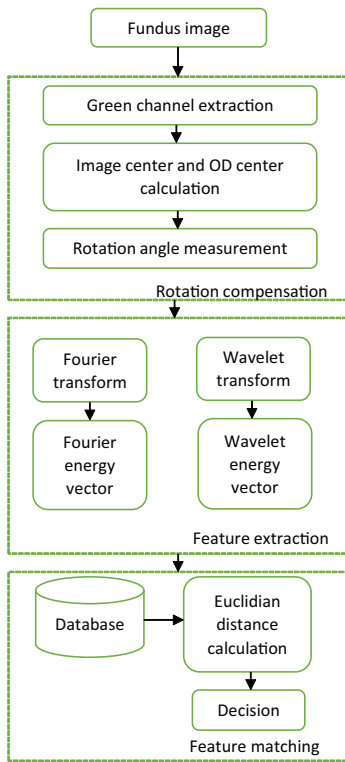


Fig. 9. Flow diagram of algorithm proposed by Sabaghi et al. [22] (2012)

database in FT, WT, and combined FT and WT methods, respectively.

Fig.10 shows the flow diagram for person identification method which use rotation invariant proposed by Dehghani et al. [23]. Authors have observed that the corners of fundus image are rotation invariant and results in better recognition. Harris corner detector is used to extract the corners of the fundus image. The intensity change  $E$  produced by displacement  $(x_o, y_o)$  in the original image intensity  $I$  due to sliding window is computed by

$$E(x_o, y_o) = \sum_x \sum_y w_{x,y} (I_{x_o+x, y_o+y} - I_{x,y})^2, \quad (8)$$

where  $w$  is the moving window. The intensity modified image is closely related to the local autocorrelation as

$$E(x_o, y_o) = (x, y)M(x, y)^T, \quad (9)$$

where  $M$  represents a symmetric matrix. The regions where both eigenvalues are large are identified as corners. The phase correlation method is used to determine the rotation angle of the head or eye movement. Then the similarity index is calculated in the final feature matching phase. A success rate of 100% is obtained for both DRIVE and STARE databases.

Fourier-Mellin transform (FMT) and Fuzzy clustering are used by Hamid et al. [24] for person identification. The unwanted rotation is compensated by finding desired rotation compensation. To obtain this, image center and optic disc center is calculated in the pre-processing stage. The initial contour required for snake model is obtained by applying Haar wavelet in three levels on the input image. The blood vessels

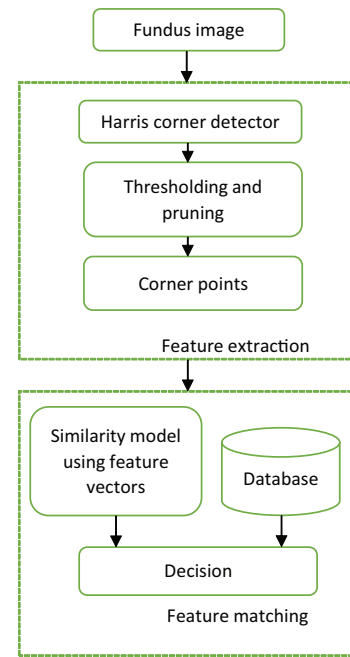


Fig. 10. Flow diagram of algorithm proposed by Dehghani et al. [23] (2013)

are removed by morphological operations and optic disc center is located by the snake model.

Fourier-Mellin transform is used to investigate the image similarity due to its invariance property. It is defined by

$$M_f(u, v) = \frac{1}{2\pi} \int_0^\infty \int_0^{2\pi} f(r, \theta) r^{-ju} \exp^{-jv\theta} d\theta \frac{dr}{r}, \quad (10)$$

where  $f(r, \theta)$  is the polar representation of the image  $f(x, y)$ . The similarity transformation in the original domain is converted into complex multiplication in the Fourier-Mellin domain by applying FMT. The central FMT harmonics contains the valuable image information. The complex moments are calculated using

$$C_{pq} = \sum_{x=0}^M \sum_{y=0}^N (x + iy)^p (x - iy)^q f(x, y), \quad (11)$$

where  $f(x, y)$  is the density distribution function and  $C_{pq}$  is the  $(p+q)^{th}$  order moments. The final feature vector is formed by combining both the extracted features. Feature matching is done by designing a classifier based on unsupervised fuzzy c-means algorithm (FCM) which minimizes the weighted sum within group sum of squared error objective function, given by

$$J_m = \sum_{l=1}^q \sum_{k=1}^c u_{kl}^m \|\epsilon_l - v_k\|^2, \quad (12)$$

where  $u_{kl}$  represents the fuzzy membership of  $\epsilon_l$  with respect to cluster  $k$ ,  $c$  is the number of clusters,  $q$  is the number of data items,  $v_k$  is the center of  $k^{th}$  cluster,  $\|\epsilon_l - v_k\|^2$  is the distance measure between object  $\epsilon_l$  and cluster  $v_k$ , and  $m$  is the constant. They have obtained an error rate close to zero for a large range of threshold value in the local database consisting of 37 images.

TABLE II  
COMPARISON OF NON-VASCULAR BASED METHODS FOR PERSON IDENTIFICATION

Author	Image processing techniques	Database	Performance measure (%)
Rahman et al. [21], (2008)	Background elimination, contrast enhancement, Statistical and texture feature extraction, Euclidian distance measure	Local	AC: 94.5
Sabaghi et al. [22], (2012)	Template matching, Fourier transform, Wavelet transform, Euclidian distance measure	DRIVE	RR: 99.1
Dehghani et al. [23], (2013)	Harris corner detector, phase correlation, similarity score	DRIVE STARE	RR: 100 RR: 100
Hamid et al. [24], (2014)	Active contour, Fourier-Mellin transform fuzzy c-means clustering	Local	EER $\simeq$ 0
Waheed et al. [25], (2016)	Structural properties like luminance, contrast and structure extraction, similarity score measure	RIDB AFIO	RR: 92.5 RR: 85.75
Modarresi et al. [26], (2017)	Template matching, Shearlets transform, Mahalanobis distance measure	DRIVE STARE Local	EER: 0.11 EER: 0.18 EER: 0.24
Modarresi et al. [27], (2018)	Template matching, contourlet transform Mahalanobis distance measure	Local	EER : 0.32

Waheed et al. [25] have proposed a fast and simple non-vascular based person identification system consists of two phases. In the first phase, structural properties like luminance, contrast, and structure are extracted. A local window of size  $8 \times 8$  is used to compute the required features. The mean and standard deviation of images to be compared are computed. The luminance and contrast are measured from the calculated values using the following equations

$$L(x, y) = \frac{2\mu_x\mu_y + C_1}{\mu_x^2 + \mu_y^2 + C_1}, \quad (13)$$

$$C(x, y) = \frac{2\sigma_x\sigma_y + C_1}{\sigma_x^2 + \sigma_y^2 + C_1}, \quad (14)$$

where  $C_1$  is constant,  $\mu_x$ ,  $\mu_y$ ,  $\sigma_x$ , and  $\sigma_y$  represents the mean intensity and standard deviation for two input images  $x$  and  $y$ , respectively. The structure measurement is done by combining the luminance and contrast functions. The image is normalized by its standard deviation and the structure function is calculated using

$$S(x, y) = \frac{2\sigma_{xy} + C_1}{\sigma_x\sigma_y + C_1}. \quad (15)$$

The parameter  $\sigma_{xy}$  can be calculated by

$$\sigma_{xy} = \left( \frac{1}{N-1} \left[ \sum_{i=1}^N (x_i - \mu_x)(y_i - \mu_y) \right] \right)^{\frac{1}{2}}. \quad (16)$$

A local similarity score between two images is computed by combining the measured features using

$$Simscore(x, y) = [L(x, y)]^\alpha \cdot [C(x, y)]^\beta \cdot [S(x, y)]^\gamma, \quad (17)$$

where  $\alpha > 0$ ,  $\beta > 0$ , and  $\gamma > 0$  are the adjusting parameters. The overall similarity score is given by

$$Meansimscore(X, Y) = \frac{1}{M} \sum_{j=1}^M Simscore(x_j, y_j), \quad (18)$$

where  $X$  and  $Y$  denotes two images,  $x_j$  and  $y_j$  are image contents at  $j_{th}$  local window, and  $M$  represents the number of local windows in an image. Identification of person is obtained based on the highest score value. Authors have tested their algorithm on RIDB and AFIO databases and achieved the recognition rate of 92.5% and 85.75%, respectively with reduced processing time.

Modarresi et al. [26] have proposed an automated person identification method using Shearlets transform. Rotation compensation, OD localization, and ROI identification are performed in the pre-processing stage. The head or eye movement during image acquisition is compensated by calculating the desired rotation angle. To achieve this, a method based on Radial Tchebichef Moments [28] is employed. The optic disc center is located using template matching technique, where correlation between the retinal image and template is computed by

$$R(i, j) = \frac{\sum_k \sum_l (f_{k+i, l+j} - \bar{f}_{i, j})(t_{k, l} - \bar{t})}{\left[ \left( \sum_k \sum_l (f_{k+i, l+j} - \bar{f}_{i, j})^2 \right) \left( \sum_k \sum_l (t_{k, l} - \bar{t})^2 \right) \right]^{0.5}}, \quad (19)$$

where  $R(i, j)$  is the normalized correlation coefficient (CC),  $f$  is the original image,  $t$  is the template,  $\bar{f}$  is the mean value of the image, and  $\bar{t}$  is the mean value of the template. The brightest point in the correlated image is taken as OD focal point. This is followed by ROI extraction, which results in a rotation invariant image. Multi-resolution analysis [29] method

based on Shearlets transform is used in feature extraction stage. Signal singularities such as edges can be precisely detected and located in images. Shearlet transform of  $I$  is defined as

$$SH_{\Phi}I(a, s, t) = \langle I, \Phi_{a,s,t} \rangle, a > 0, s \in R, t \in R^2. \quad (20)$$

The shearlet basis function  $\Phi_{a,s,t}$  is given by

$$\Phi_{a,s,t}(x) = |\det M_{a,s}|^{-\frac{1}{2}} \Phi(M_{a,s}^{-1}x - t), \quad (21)$$

where  $M_{a,s} = (B_s A_a)$ ,  $A_a$  is the anisotropic dilation matrix and  $B_s$  is the shear matrix. Several statistical texture features such as correlation, entropy, uniformity, dissimilarity, and cluster shade are extracted by applying 2D Shearlets transform [30]. A feature vector is created based on the extracted features. In matching phase, the distance score between the test image  $x$  and the stored image  $z$  is computed by Mahalanobis distance using

$$d_M(x, z) = \sqrt{(x - z)^T \cdot (\Sigma(x - z))^{-1}}, \quad (22)$$

where  $\Sigma$  is a covariance matrix defined by

$$\Sigma = cov(x, z) = E \left[ (x - E[z]) \cdot (x - E[z])^T \right]. \quad (23)$$

The method is tested on DRIVE, STARE, and local databases and noted equal error rate (EER) of 0.11%, 0.18%, and 0.24%, respectively.

A robust three stage person identification system using human retina is proposed by Modarresi et al. [27]. Pre-processing is the first stage and it includes rotation compensation, OD localization, and ROI identification. In order to enhance the system performance, rotation compensation and scale invariant method based on Radial Tchebichef Moments are introduced. A template matching method is used for OD localization. The point with highest CC value defined in Equation (19) is considered as OD center point. A circular area with 500 pixels diameter at a distance of 50 pixels from the reference point is selected for ROI identification. In feature extraction stage, image decomposition at different scales is performed by Contourlet transform [31]. Contourlet transform is an extension of the wavelet transform which incorporates multi-scale and directional filter bank (DFB). Multi-scale decomposition is achieved by Laplacian pyramid (LP). The LP decomposition within each level generates a lowpass and bandpass images. The directional information is efficiently captured by performing directional decomposition using directional filter bank. Statistical features such as mean energy, standard deviation, information entropy, contrast, and homogeneity are extracted from each sub-images. A feature vector of each sub-image is created based on the extracted features. By combining the feature vectors of all sub-images, the final feature vector is generated. Finally, the similarity score based on Mahalanobis distance given in Equation (22) is calculated in the matching phase. The algorithm is tested on local database and an equal error rate of 0.32% is obtained.

Table II describes the results obtained considering the feature points extracted from the original color fundus image. Dehghani et al. [23] has obtained the recognition rate of 100%

in DRIVE and STARE databases using non-vascular based method for person identification.

### C. Discussion on Retinal Database and Performance measures

Most of the person identification methods presented in the literature are tested on various publicly available databases. The efficiency of various methods have been evaluated by different performance measures [32] such as accuracy (AC), recognition rate (RR), false rejection rate (FRR), false acceptance rate (FAR), equal error rate (ERR), precision (PR), and recall (RE) etc. A brief description of retinal databases and performance measures are provided below.

1) *Retinal Databases*: Most commonly used databases by the researchers are DRIVE, STARE, RIDB, DRIDB, AFIO, ARIA, VARIA, and SiMES etc. Some authors have tested their algorithms using local databases from the hospitals.

*DRIVE Dataset*: The Digital Retinal Images for Vessel Extraction (DRIVE) dataset [33] includes 40 color fundus images with a resolution of  $768 \times 584$  pixels. A Canon CR5 nonmydriatic 3CCD camera with a 45-degree field of view (FOV) is used to obtain the images. This dataset consists of 33 normal images and 7 pathological images. The images are classified into two groups: training set and test set each containing 20 images. Ground truth information of blood vessels is also included in this dataset.

*STARE Dataset*: The Structured Analysis of Retina (STARE) dataset [34] includes 400 color fundus images with a resolution of  $700 \times 605$ . A TopCon TRV-50 fundus camera with a 35-degree field of view is used to capture the images. Ground truth information of blood vessels is available for 40 images. The optic nerve head (ONH) is localized for 80 images.

*ARIA Dataset*: Automatic Retinal Image Analysis (ARIA) [35] is the largest database for vessel extraction. It includes 138 images with a resolution of  $768 \times 576$  pixels. These images are taken either from healthy subjects, diabetics or from patients with age-related macular degeneration (AMD). All of these images are collected with a Zeiss FF450 fundus camera at 50-degree field of view.

*RIDB Dataset*: The Retinal Identification Database (RIDB) [36], [25] is mainly used for retinal recognition. It consists of 100 healthy color fundus images collected from a local hospital. This database includes 20 individuals with 5 images per person. A TopCon TRC 50EX camera with a resolution of  $1500 \times 1000$  is used to capture the images.

*DRIDB Dataset*: The Diabetic retinopathy image database (DRIDB) [37] is a public database which includes 50 bitmap (BMP) images. Ground truth information of retinal features such as microaneurysms, hemorrhages, hard exudates, soft exudates, blood vessels, optic disk, and macula are included in the dataset. The images are captured at a resolution of  $720 \times 576$  using a ZEISS VISUCAM 200 fundus camera at 45-degree field of view.

*AFIO Dataset*: This database has been acquired by Armed Forces Institute of Ophthalmology (AFIO), Pakistan [11]. It includes 42 images collected from 14 individuals. All the

images are compressed in JPEG format with a resolution of  $1504 \times 1000$ .

**VARIA Dataset:** VARIA dataset [38], [39] consists of 233 color fundus images collected from 139 individuals. A TopCon nonmydriatic NW-100 camera is used to acquire the images. The images are optic disc centered with a resolution of  $768 \times 584$ .

**SiMES Dataset:** Singapore Malay Eye Study (SiMES) dataset [19] includes 3280 images with a resolution of  $2048 \times 3072$  pixels. These images are captured using Canon CRDGI retinal fundus camera at 45-degree field of view.

Among the retinal databases, DRIVE database is widely used by various authors. It provides better recognition rate compared to other databases.

2) **Performance Measures:** Different performance measures are used in the literature to evaluate the efficiency of person identification algorithms. Some of the performance measures are discussed below.

**Recognition Rate (RR):** It represents the percentage of correctly identified images and is given by

$$RR = \frac{n}{N}, \quad (24)$$

where  $n$  represents number of matched images and  $N$  is the total number of images.

**False Acceptance Rate (FAR):** The percentage of invalid inputs accepted correctly is false acceptance rate, given by

$$RR = \frac{fa}{T_i}, \quad (25)$$

where  $fa$  denotes total false acceptances and  $T_i$  represents total identification attempts.

**False Rejection Rate (FRR):** It refers to the percentage of valid inputs rejected incorrectly and is given by

$$RR = \frac{fr}{T_i}, \quad (26)$$

where  $fr$  denotes total false acceptances and  $T_i$  represents total identification attempts.

**Equal Error Rate (EER):** It is an ideal rate, normally used to decide the general accuracy of the framework.

**Precision (PR):** It is the ratio of correctly predicted positive observations to the total predicted positive observations, defined by

$$PR = \frac{TP}{(TP + FP)}, \quad (27)$$

where  $TP$  represents true positive and  $FP$  is false positive.

**Recall (RE):** Recall is the ratio of correctly predicted positive observations to the total observations and is given by

$$PR = \frac{TP}{(TP + FN)}, \quad (28)$$

where  $TP$  represents true positive and  $FN$  is false negative.

### III. CONCLUSION

Biometric authentication using retinal fundus image has captured the interest of many researchers due to its stability and uniqueness. Retinal blood vessel patterns play a major role in person identification. The techniques incorporating vascular features require blood vessel segmentation and more computation time. Person identification methods using non-vascular features does not require blood vessel segmentation. Hence computational complexity for implementation of these algorithms is low compared to other vascular-based methods. Even though there are many effective algorithms available in the literature, still there is a place to improve the performance of person identification method in presence of other pathologies.

In this paper, a comprehensive review of person identification using fundus image are discussed and compared based on the performance measures such as accuracy, false acceptance rate, false rejection rate, equal error rate, precision, and recall to provide the researchers about the methods available till date for person identification. Traditional methods of person identification are covered first, followed by the comparison of various algorithms in terms of performance measures. Among the available methods in literature Jiu et al., Fatima et al., Dehghani et al., and Modarresi et al. perform better compared to other methods with different public databases.

### REFERENCES

- [1] S. Pal, U. Pal, and M. Blumenstein, "Signature-based biometric authentication," *Studies in Computational Intelligence*, vol. 555, pp. 285–314, Jan. 2014.
- [2] M. M. H. Ali, V. H. Mahale, P. Yannawar, and A. T. Gaikwad, "Overview of fingerprint recognition system," in *2016 International Conference on Electrical, Electronics, and Optimization Techniques (ICEEOT)*, pp. 1334–1338, Mar. 2016.
- [3] H. Shah, M. Ab Rashid, M. F. Abdollah, M. N. Kamarudin, C. Lin, and Z. Kamis, "Biometric voice recognition in security system," *Indian Journal of Science and Technology*.
- [4] J. Soldera, G. Schu, L. R. ScharDOSim, and E. T. Beltrao, "Facial biometrics and applications," *IEEE Instrumentation Measurement Magazine*, vol. 20, pp. 4–30, April 2017.
- [5] J. Liu-Jimenez, R. Sanchez-Reillo, and B. Fernandez-Saavedra, "Iris biometrics for embedded systems," *IEEE Transactions on Very Large Scale Integration (VLSI) Systems*, vol. 19, pp. 274–282, Feb 2011.
- [6] Z. Zhou, E. Y. Du, N. L. Thomas, and E. J. Delp, "A new human identification method: Sclera recognition," *IEEE Transactions on Systems, Man, and Cybernetics - Part A: Systems and Humans*, vol. 42, pp. 571–583, May 2012.
- [7] C. Simon and I. Goldstein, "A new scientific method of identification," *New York State Journal of Medicine*, vol. 35, no. 18, pp. 901–906, 1955.
- [8] P. Tower, "The fundus oculi in monozygotic twins: report of six pairs of identical twins," *Archives of Ophthalmology*, vol. 54, pp. 225–239, 1955.
- [9] A. K. Jain, A. Ross, and S. Prabhakar, "An introduction to biometric recognition," *IEEE Transactions on circuits and systems for video technology*, vol. 14, no. 1, pp. 4–20, 2004.
- [10] E. Poonguzhali, R. Giritharan, M. K. Nath, and O. P. Acharya, "Review on localization of optic disc in retinal fundus images," in *International Conference on Applied Electromagnetics, Signal Processing and Communication (AESPC)*, Oct. 2018.
- [11] Z. Waheed, M. U. Akram, A. Waheed, M. A. Khan, A. Shaukat, and M. Ishaq, "Person identification using vascular and non-vascular retinal features," *Computers and Electrical Engineering*, vol. 53, pp. 359 – 371, 2016.

- [12] S. Moccia, E. D. Momi, S. E. Hadji, and L. S. Mattos, "Blood vessel segmentation algorithms review of methods, datasets and evaluation metrics," *Computer Methods and Programs in Biomedicine*, vol. 158, pp. 71 – 91, 2018.
- [13] H. Farzin, H. Abrishami-Moghaddam, and M.-S. Moin, "A novel retinal identification system," *EURASIP Journal on Advances in Signal Processing*, vol. 2008, Apr. 2008.
- [14] M. Akram, A. Tariq, and S. Khan, "Retinal recognition: Personal identification using blood vessels," *2011 International Conference for Internet Technology and Secured Transactions, ICITST 2011*.
- [15] J. Fatima, A. M. Syed, and M. Akram, "A secure personal identification system based on human retina," in *ISIEA 2013 - 2013 IEEE Symposium on Industrial Electronics and Applications*, pp. 90–95, Sep. 2013.
- [16] R. K. Gharami and M. K. Nath, "A new approach to biometric person identification from retinal vascular patterns," *Emerging Trends and Technology in Computer Science (IJETTCS)*, vol. 3, pp. 191–195, Sep. 2014.
- [17] Z. Waheed, M. U. Akram, A. Waheed, M. A. Khan, A. Shaukat, and M. Ishaq, "Person identification using vascular and non-vascular retinal features," *Computers and Electrical Engineering*, vol. 53, 2016.
- [18] F. Jiu, K. Noronha, and D. Jayaswal, "Biometric identification through detection of retinal vasculature," *2016 IEEE 1st International Conference on Power Electronics, Intelligent Control and Energy Systems (ICPEICES)*, pp. 1–5, 2016.
- [19] A. Bhuiyan, A. Hussain, A. Mian, T. Y. Wong, K. Ramamohanarao, and Y. Kanagasigam, "Biometric authentication system using retinal vessel pattern and geometric hashing," *IET Biometrics*, vol. 6, no. 2, pp. 79–88, 2017.
- [20] U. T. V. Nguyen, A. Bhuiyan, L. A. F. Park, and K. Ramamohanarao, "An effective retinal blood vessel segmentation method using multi-scale line detection," *Pattern Recognition*, vol. 46, no. 3, pp. 703 – 715, 2013.
- [21] N. A. Rahman, A. S. Mohamed, and M. E. Rasmay, "Retinal identification," in *2008 Cairo International Biomedical Engineering Conference*, pp. 1–4, Dec. 2008.
- [22] M. Sabaghi, S. R. Hadianamrei, M. Fattahi, M. R. Kouchaki, and A. Zahedi, "Retinal identification system based on the combination of fourier and wavelet transform," *Journal of Signal and Information Processing*, vol. 03, no. 01, 2012.
- [23] A. Dehghani, Z. Ghassabi, H. A. Moghddam, and M. S. Moin, "Human recognition based on retinal images and using new similarity function," *EURASIP Journal on Image and Video Processing*, vol. 2013, Oct. 2013.
- [24] H. Tabatabaee and H. Jafariani, "Retinal identification system using fourier-mellin transform and fuzzy clustering," *Indian Journal of Science and Technology*.
- [25] Z. Waheed, A. Waheed, and M. U. Akram, "A robust non-vascular retina recognition system using structural features of retinal image," in *2016 13th International Bhurban Conference on Applied Sciences and Technology (IBCAST)*, pp. 101–105, Jan. 2016.
- [26] M. Modarresi, I. S. Oveisi, and M. Janbozorgi, "Retinal identification using shearlets feature extraction," *Austin Biometrics and Biostatistics*, vol. 4, 2017.
- [27] M. M. Asem and I. S. Oveisi, "Biometric retinal authentication based on multi-resolution feature extraction using mahalanobis distance," *Biometrics and Biostatistics International Journal*.
- [28] R. Mukundan, S. H. Ong, and P. A. Lee, "Image analysis by tchebichef moments," *IEEE Transactions on Image Processing*, vol. 10, pp. 1357–1364, Sep. 2001.
- [29] M. K. Nath and S. Dandapat, "Differential entropy in wavelet sub-band for assessment of glaucoma," *International Journal of Imaging Systems and Technology*, vol. 22, no. 03, 2012.
- [30] W.-Q. Lim, "The discrete shearlet transform: A new directional transform and compactly supported shearlet frames," *IEEE Transactions on Image Processing*, vol. 19, pp. 1166–1180, May. 2010.
- [31] M. N. Do and M. Vetterli, "The contourlet transform: an efficient directional multiresolution image representation," *IEEE Transactions on Image Processing*, vol. 14, pp. 2091–2106, Dec 2005.
- [32] R. Giritharan, E. Poonguzhali, and M. K. Nath, "Diagnosis of retinitis pigmentosa from retinal images," *International Journal of Electronics and Telecommunications*, vol. 65, no. 3, pp. 519 – 525, 2019.
- [33] J. Staal, M. D. Abramoff, M. Niemeijer, M. A. Viergever, and B. van Ginneken, "Ridge-based vessel segmentation in color images of the retina," *IEEE Transactions on Medical Imaging*, vol. 23, pp. 501–509, April 2004.
- [34] A. Hoover and M. Goldbaum, "Locating the optic nerve in a retinal image using the fuzzy convergence of the blood vessels," *IEEE Transactions on Medical Imaging*, vol. 22, pp. 951–958, Aug 2003.
- [35] D. J. J. Farnell, F. N. Hatfield, P. Knox, M. Reakes, D. Parry, and S. P. Harding, "Enhancement of blood vessels in digital fundus photographs via the application of multiscale line operators," *Journal of the Franklin Institute*, vol. 345, no. 7, pp. 748 – 765, 2008.
- [36] RIDB, "Retinal identification databases," [www.biomisa.org/RIDB](http://www.biomisa.org/RIDB).
- [37] P. Prentasac, S. Loncaric, Z. Vatauvuk, G. Bencic, M. Subasic, T. Petkovic, L. Dujmovic, M. M.-R. N. Budimlija, and R. Tadic, "Diabetic retinopathy image database(dridb): A new database for diabetic retinopathy screening programs research," in *2013 8th International Symposium on Image and Signal Processing and Analysis (ISPA)*, pp. 711–716, Sep. 2013.
- [38] M. Ortega, M. Penedo, J. Rouco, N. Barreira, and M. Carreira, "Personal verification based on extraction and characterisation of retinal feature points," *Journal of Visual Languages and Computing*, vol. 20, no. 2, pp. 80 – 90, 2009.
- [39] VARIA, "Varpa retinal images for authentication," <http://www.varpa.es/varia.html>.